

# Optimization of 3D diamond detectors with graphitized electrodes based on an innovative numerical simulation

L. Anderlini<sup>a</sup>, A. Bombini<sup>a</sup>, **Clarissa Buti**\*<sup>a,b</sup>, D. Janssens<sup>c</sup>, S. Lagomarsino<sup>b</sup>,  
Michele Veltri<sup>a,d</sup>

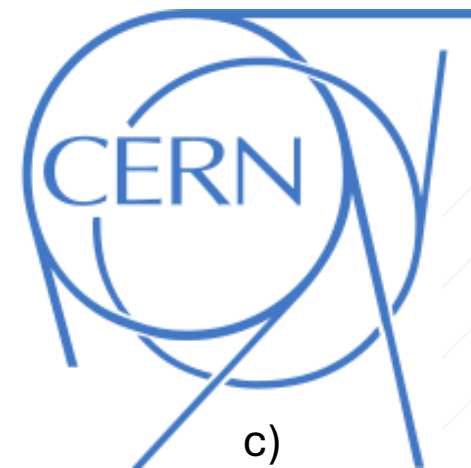


a)



b)

UNIVERSITÀ  
DEGLI STUDI  
FIRENZE



c)



d)

1506  
UNIVERSITÀ  
DEGLI STUDI  
DI URBINO  
CARLO BO

---

# OUTLINE

- 1. Why a New Simulation Approach for 3D Diamond Detectors?**
- 2. The Proposed Simulation Method**
- 3. Validation with Experimental Data**
- 4. Detector Optimization Based on the Simulation**

# DIAMOND DETECTORS

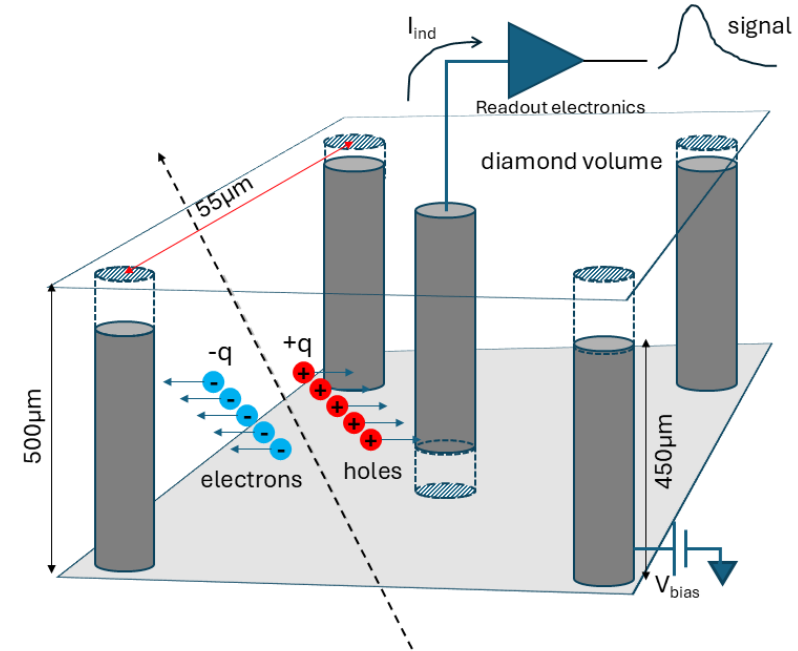
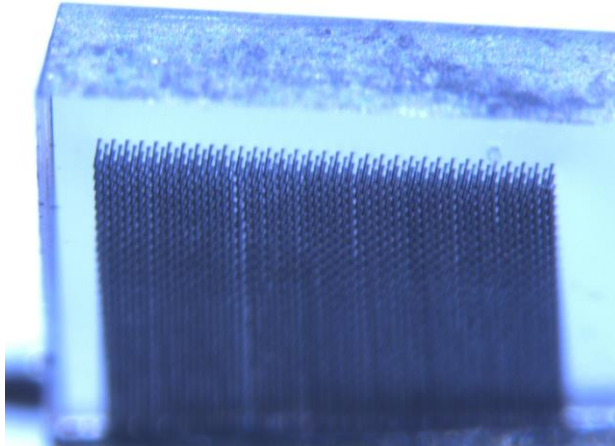
The current challenge in the field of solid-state detector development is to design devices capable of operating under extreme radiation conditions. Two key aspects must be addressed: **excellent timing performance** and **high radiation resistance**.

## DIAMOND IS AN INTERESTING CANDIDATE!

- High radiation tolerance
- High charges mobility and saturation velocity
- Solar-blind
- Operable at high temperatures
- 3D geometry thanks to graphitization

## NOT THE ONLY ONE!

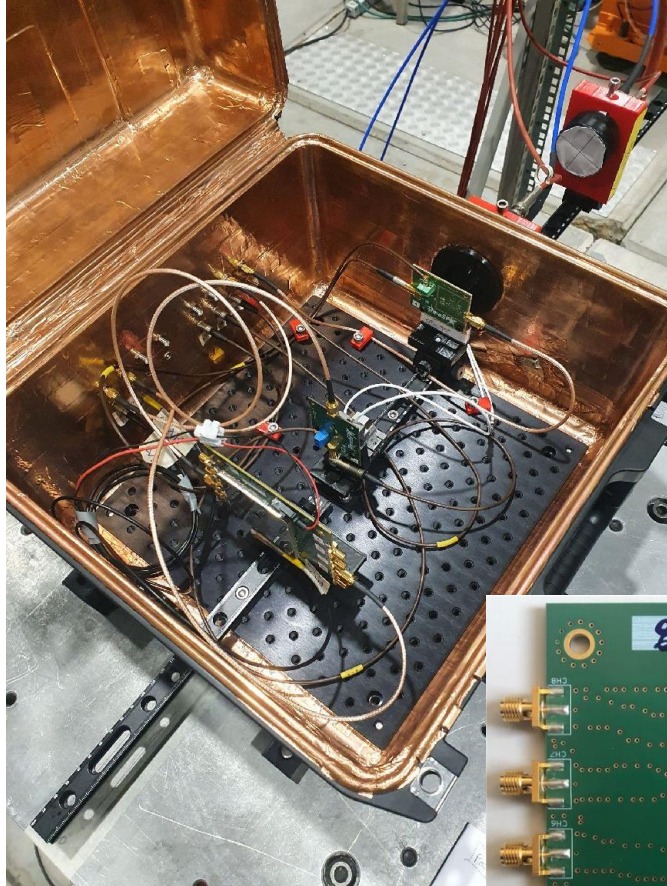
- LGAD (Valentina Sola), RF PMT (Simon Zhamkochyan), HRPPD (Alexander Kiselev) (Talks of this morning!)



Physical properties	Diamond	Silicon
Separation Energy (eV)	5.5	3.6
Electron mobility ( $\text{cm}^2/\text{V} \times \text{s}$ )	4551	1350
Hole mobility ( $\text{cm}^2/\text{V} \times \text{s}$ )	2750	480
Electron saturation velocity (cm/s)	$2.6 \times 10^7$	$10^7$
Hole saturation velocity (cm/s)	$1.6 \times 10^7$	$7.5 \times 10^6$
Limit energy of dislocation (eV)	37.5-47.6	36

# TEST BEAM 2021

A **test beam** with this type of detector was conducted in **2021 at the SPS at CERN**, during which a record time resolution of  **$(82 \pm 2)$  ps** was achieved.



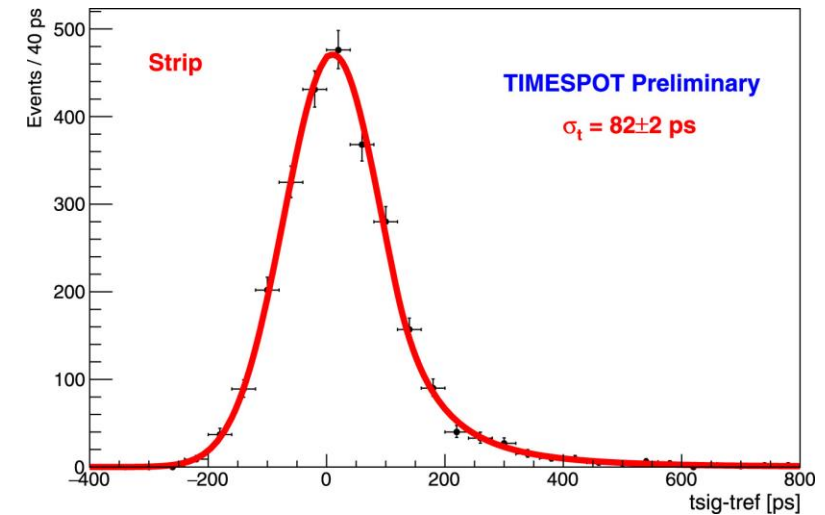
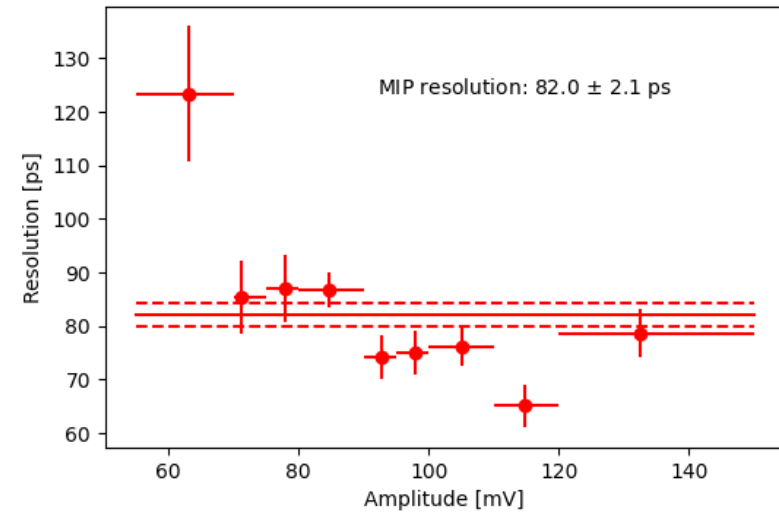
## BEAM:

- 180 GeV/c hadrons
- Gaussian angular distribution:  
 $\sigma_x = 14.9$  mrad e  $\sigma_y = 31.8$  mrad

## DETECTOR:

- Matrix 6x6 pixel  $55 \mu\text{m} \times 55 \mu\text{m}$
- Electrode resistance = 30 k $\Omega$

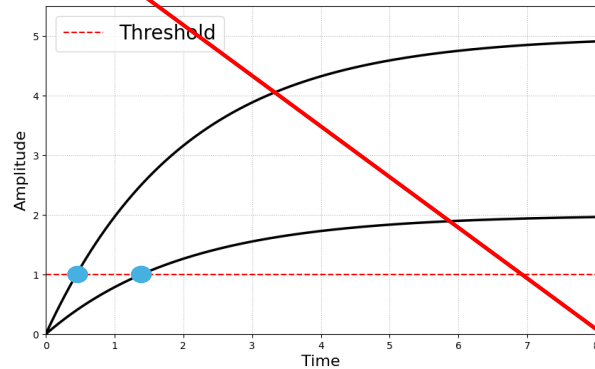
Kansas University Team  
Board



# TIME RESOLUTION

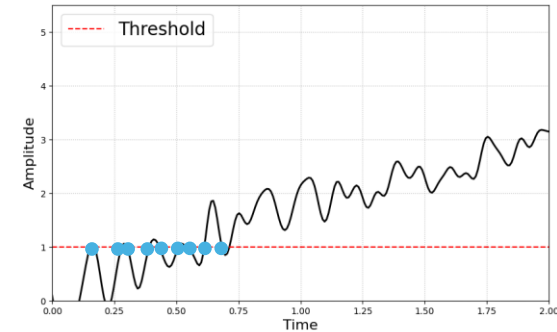
$$\sigma_{tot}^2 = \sigma_{TimeWalk}^2 + \sigma_{jitter}^2 + \sigma_{distortion}^2 + \sigma_{resistance}^2$$

## 1) $\sigma_{TimeWalk}^2$ : different amplitudes

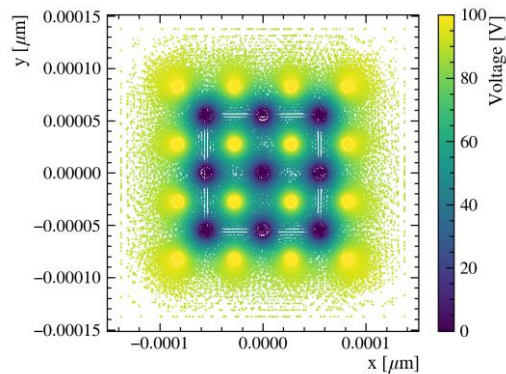


We use  
a CFD

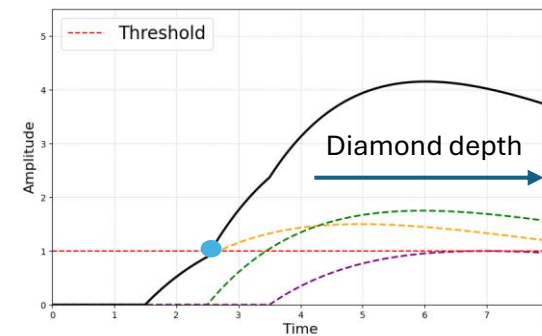
## 2) $\sigma_{jitter}^2$ : noise contribution



## 3) $\sigma_{distortion}^2$ : inhomogeneities of the electric field

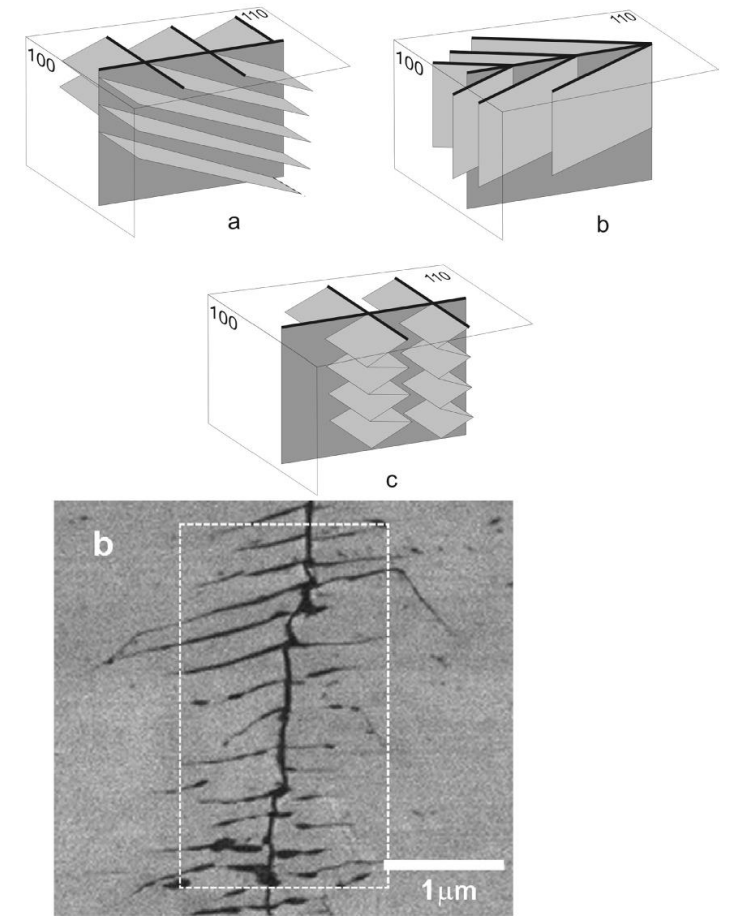
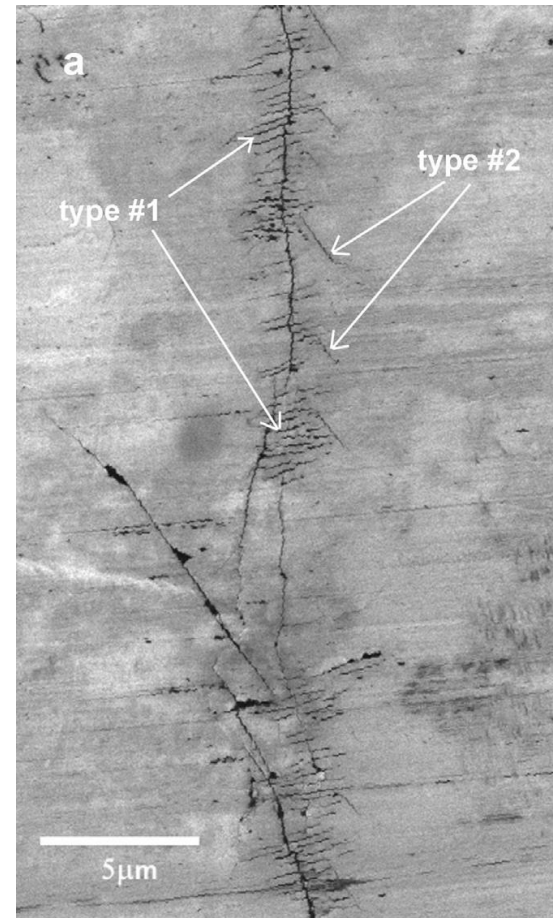
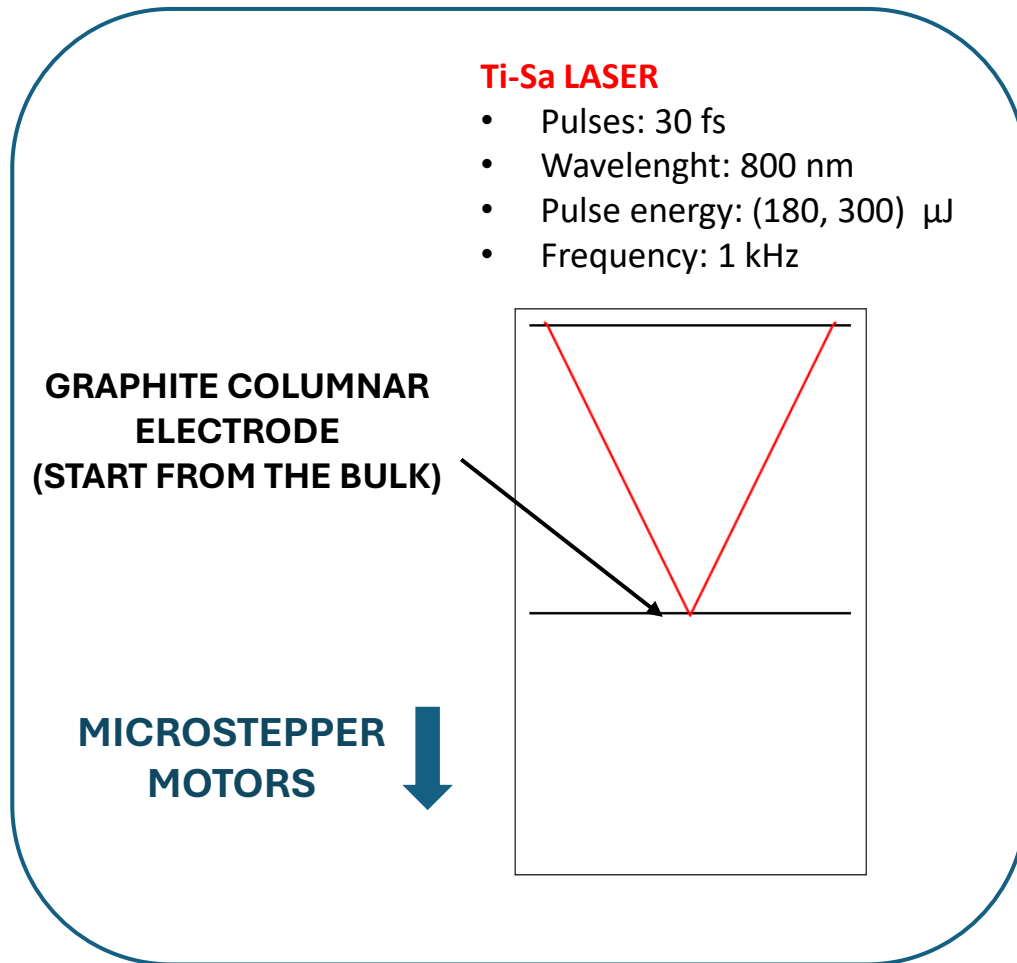


## 4) $\sigma_{resistance}^2$ : signal transmission along the resistive electrodes



# FABRICATION OF GRAPHITIZED ELECTRODES

- The **diameter** is hard to estimate, so there is **uncertainty on the resistance value**
- $\sigma_{resistance}$  **can't be neglected**



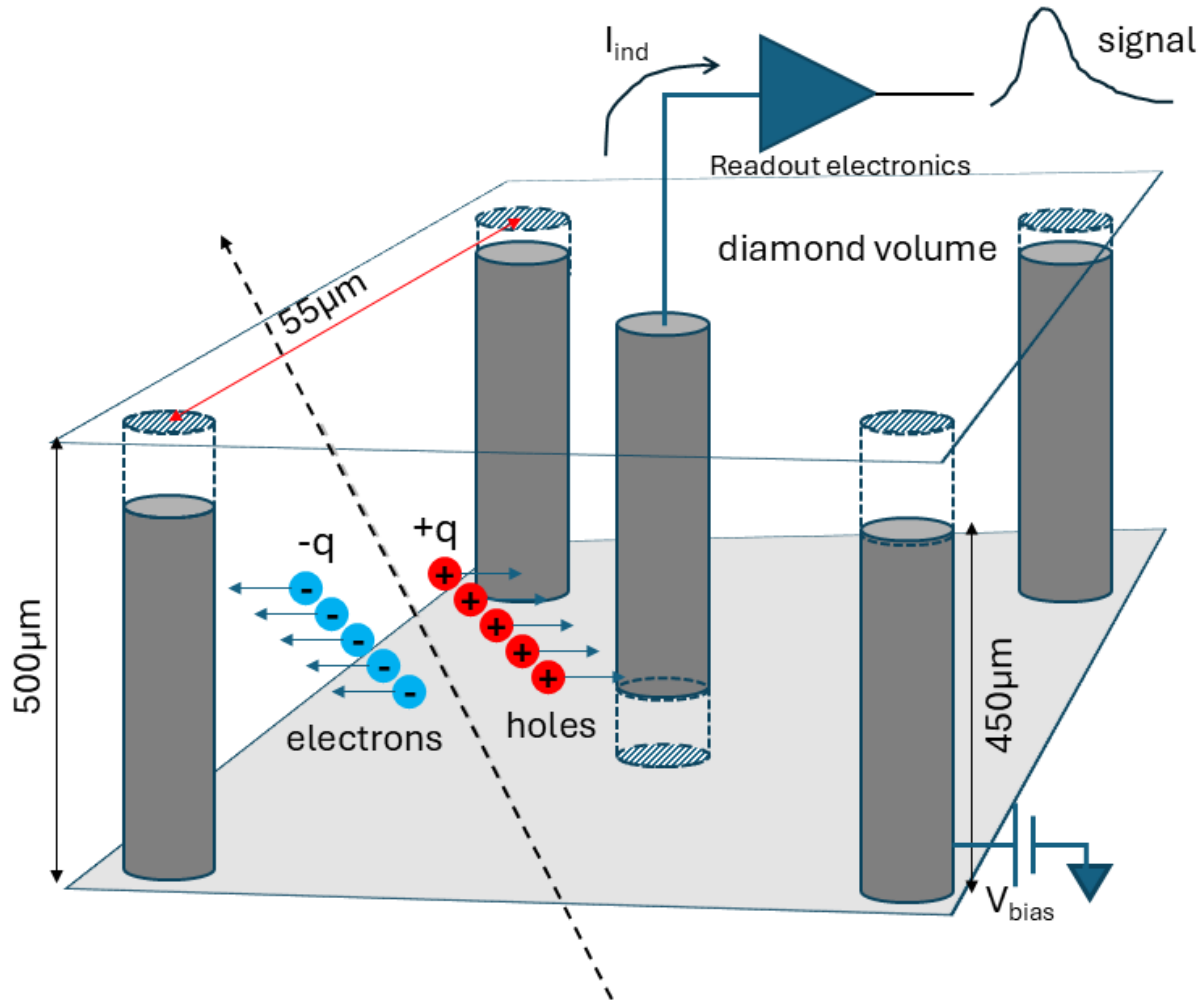
Ashikkalieva et al., *Carbon*, 102 (2016), 383–389. DOI:10.1016/j.carbon.2016.02.044

---

# **INNOVATIVE NUMERICAL SIMULATION FOR 3D DIAMOND DETECTORS**

# SIGNAL GENERATION IN THE CASE OF PERFECTLY CONDUCTIVE ELECTRODES

Output signal is generated by the motion of charge carriers in the sensor and in the case of **perfectly conductive electrodes** can be calculated through the **Ramo-Shockley theorem** using the software package **Garfield++**.



$$\vec{i}_n = \frac{q}{V_w} \vec{E}_w(\vec{x}) \cdot \vec{v}(t)$$

Assumptions to find the weighting field  $\vec{E}_{w,n}$ :

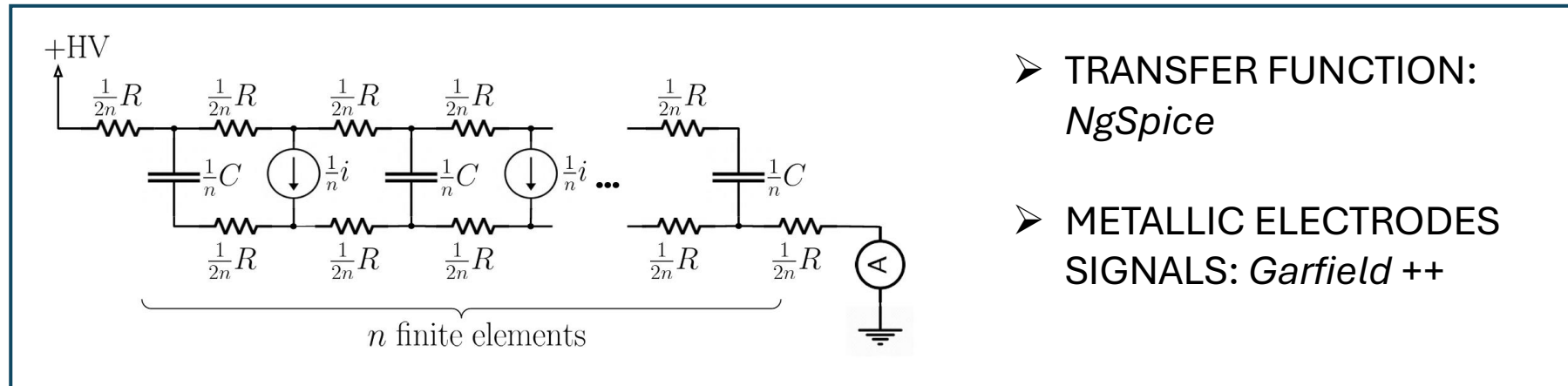
- Electrode  $n$  is at fixed voltage  $V_w$
- All the others electrodes are at zero voltage
- Any charge trapped in the volume is neglected

# SIGNAL PROPAGATION SIMULATION

To take in consideration the contribution of the electrode resistance to the signal propagation two approaches are used:

- **SIMPLE OLD APPROACH:**

**DISCRETE IMPEDANCE NETWORK:** The transfer function of the equivalent circuit is convolved numerically with the signal obtained with the assumption of metallic electrodes.



➤ TRANSFER FUNCTION:  
*NgSpice*

➤ METALLIC ELECTRODES  
SIGNALS: *Garfield ++*

## LIMITATIONS:

- Crude approximation
- Not aware of the trajectory of the ionizing particle (same response tilting the track)
- Does not allow engineering geometries

# EXTENSION OF RAMO-SHOCKLEY THEOREM

- **NOVEL APPROACH:**

**EXTENSION OF THE RAMO-SHOCKLEY THEOREM:** Effects of signal propagation due to impedance within the sensor can be modeled through a time-dependent weighting potential

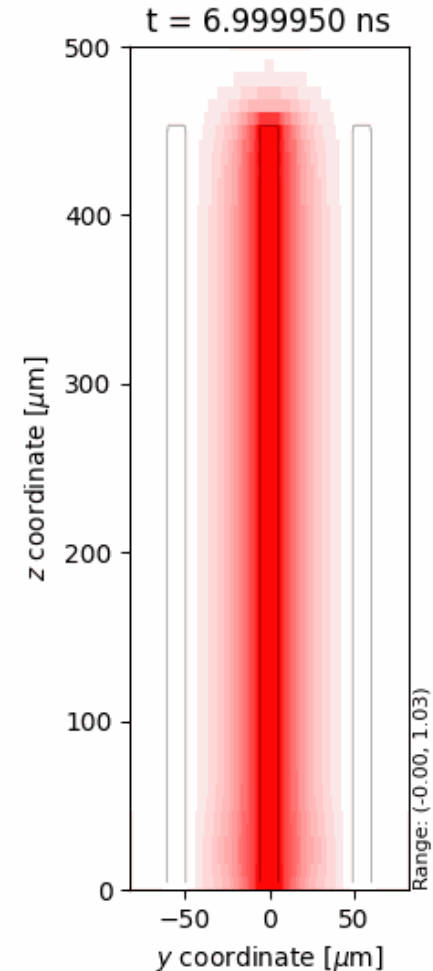
$$\vec{i}_n = \frac{q}{V_w} \int_0^t \vec{E}_w(\vec{x}, t - t') \cdot \vec{v}(t') dt'$$

**Time-dependent weighting potential:** The time-dependent weighting potential solves the Maxwell equations in the quasi-static approximation:

$$\begin{cases} \nabla^2 V(\vec{x}, t) = -\frac{\rho(\vec{x}, t)}{\epsilon} \\ \vec{\nabla} \cdot (\sigma(\vec{x}) \vec{\nabla} V(\vec{x}, t)) + \frac{\partial \rho(\vec{x}, t)}{\partial t} = 0 \end{cases}$$

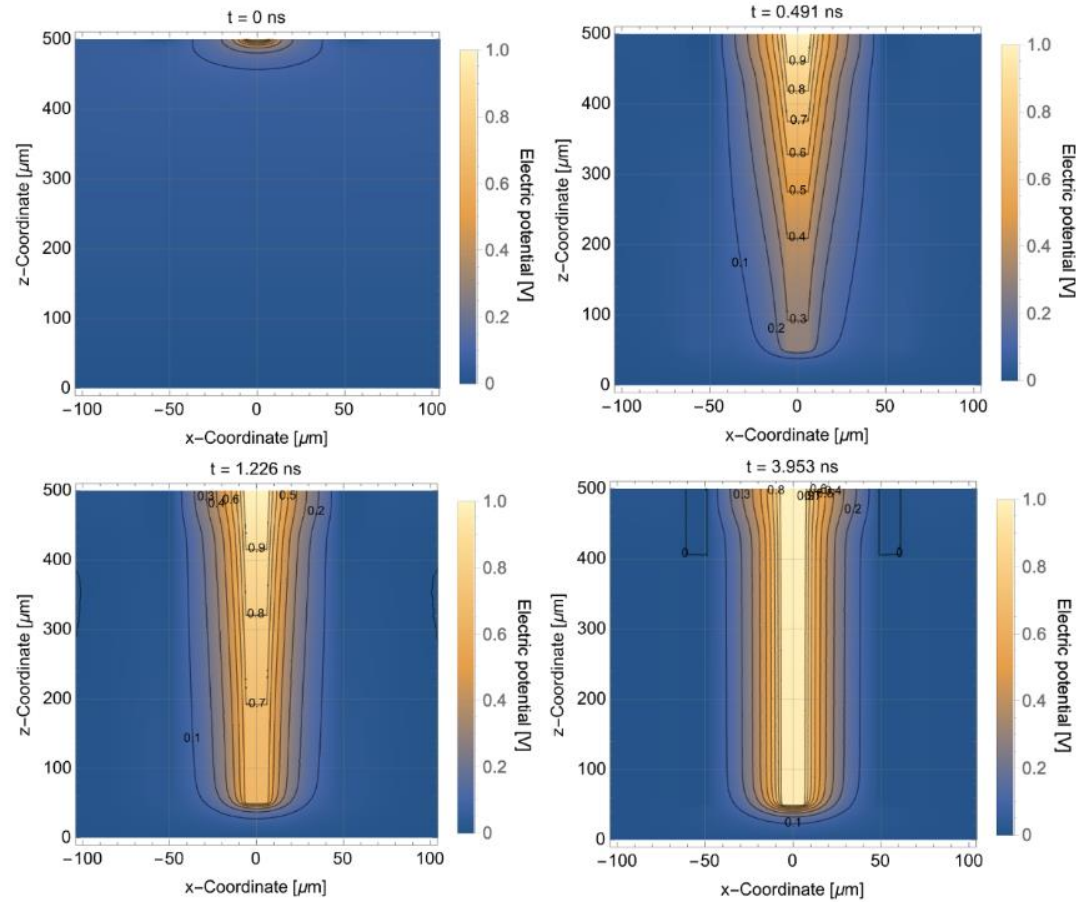
**Boundary conditions:**

- Electrode  $n$  is at fixed voltage  $V_w$
- All the others electrodes are at zero voltage



# CALCULATING THE TIME-DEPENDENT WEIGHTING POTENTIAL

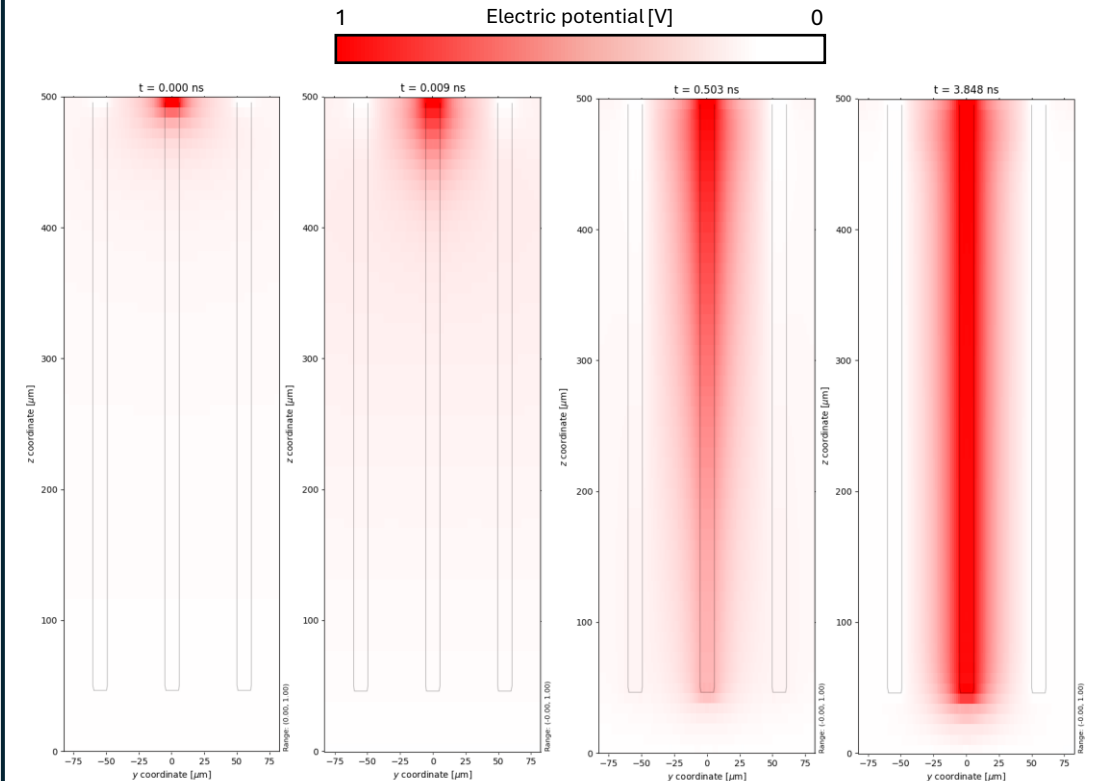
## Finite Element Method COMSOL MultiPhysics®



Janssens, Djunes. *Resistive electrodes and particle detectors: Modelling and measurements of novel detector structures*. 2024. <https://cds.cern.ch/record/2890572>

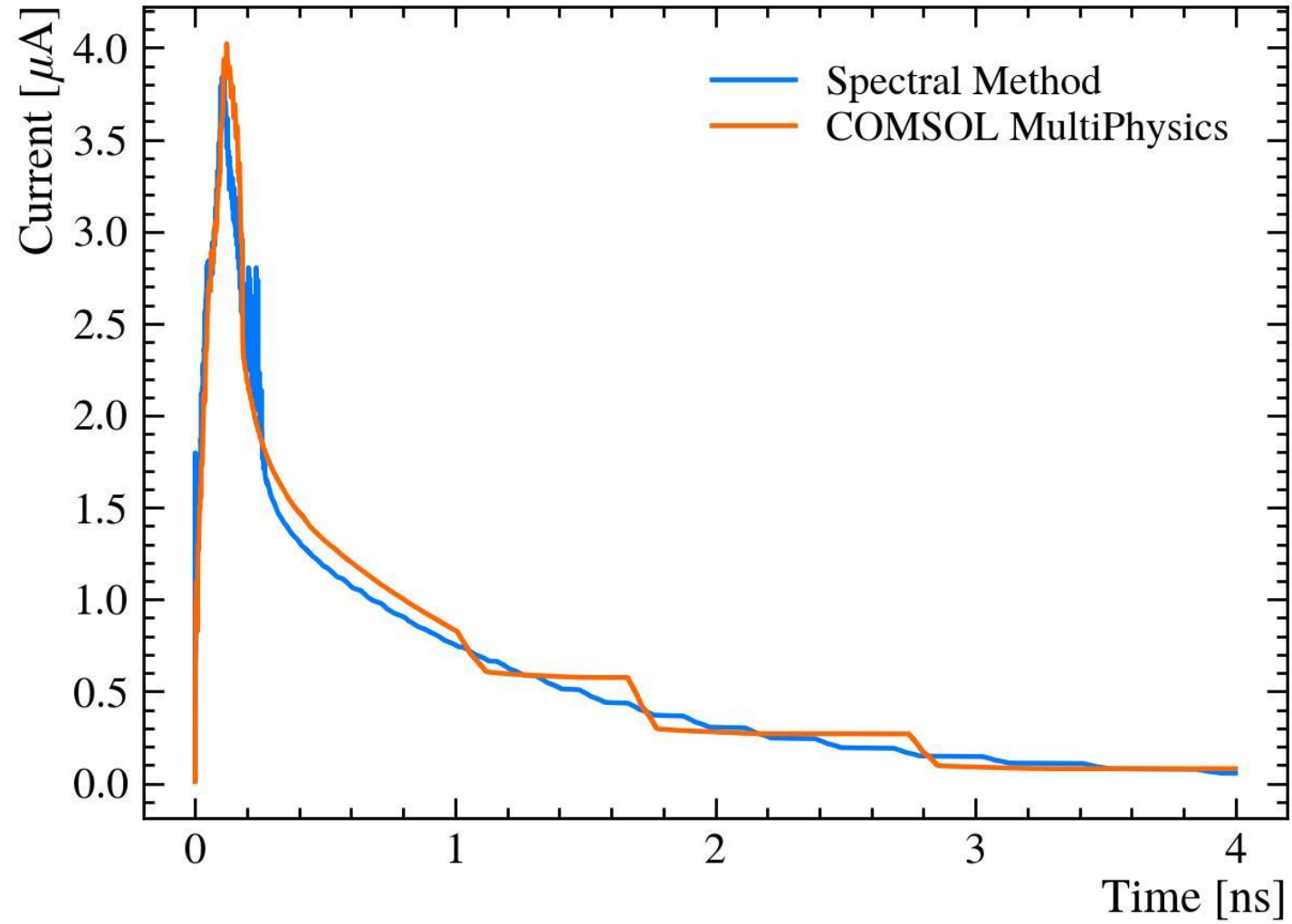
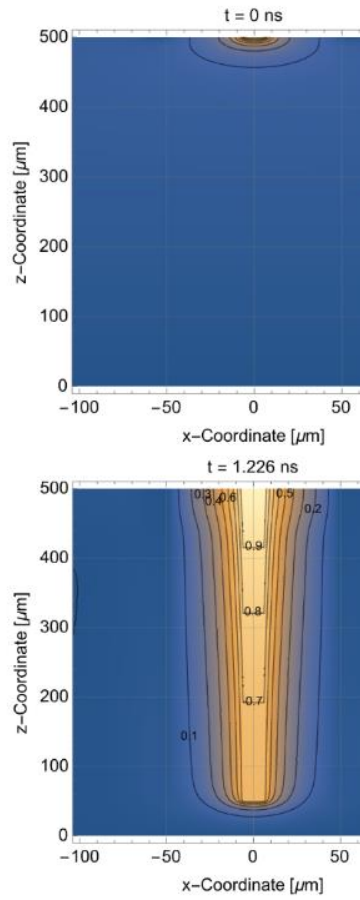
## Spectral Method

- Faster
- No need for expensive licenses
- Fast Fourier Transforms
- Fixed Voxel (120 x 120 x 64)

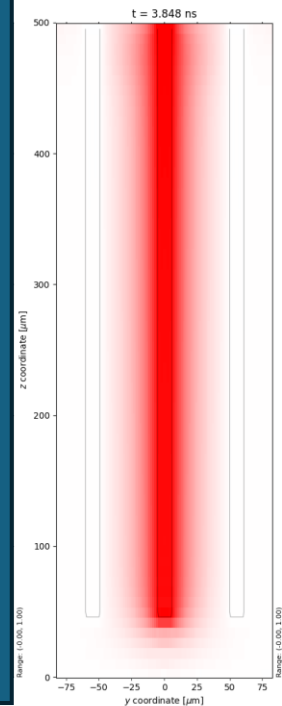


# CALCULATING THE TIME-DEPENDENT WEIGHTING POTENTIAL

Fin  
COM



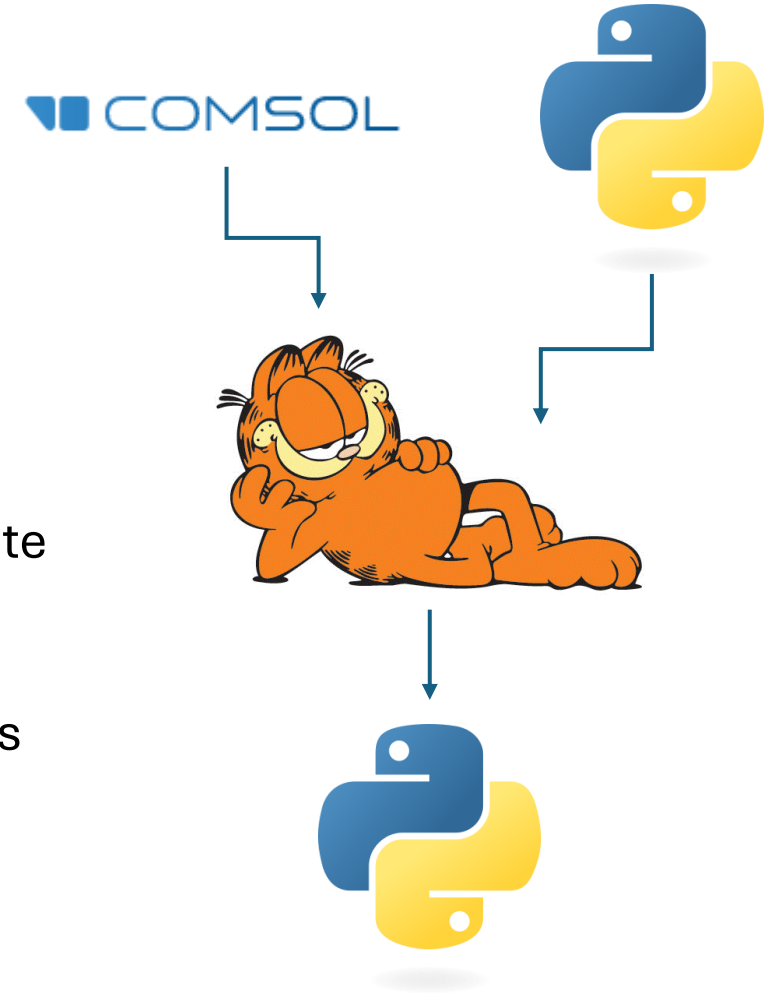
nse



Janssens, Djunes. *Resistive electro detector structures*. 2024. <https://cds.cern.ch/record/2890572>

# SIMULATION PIPELINE

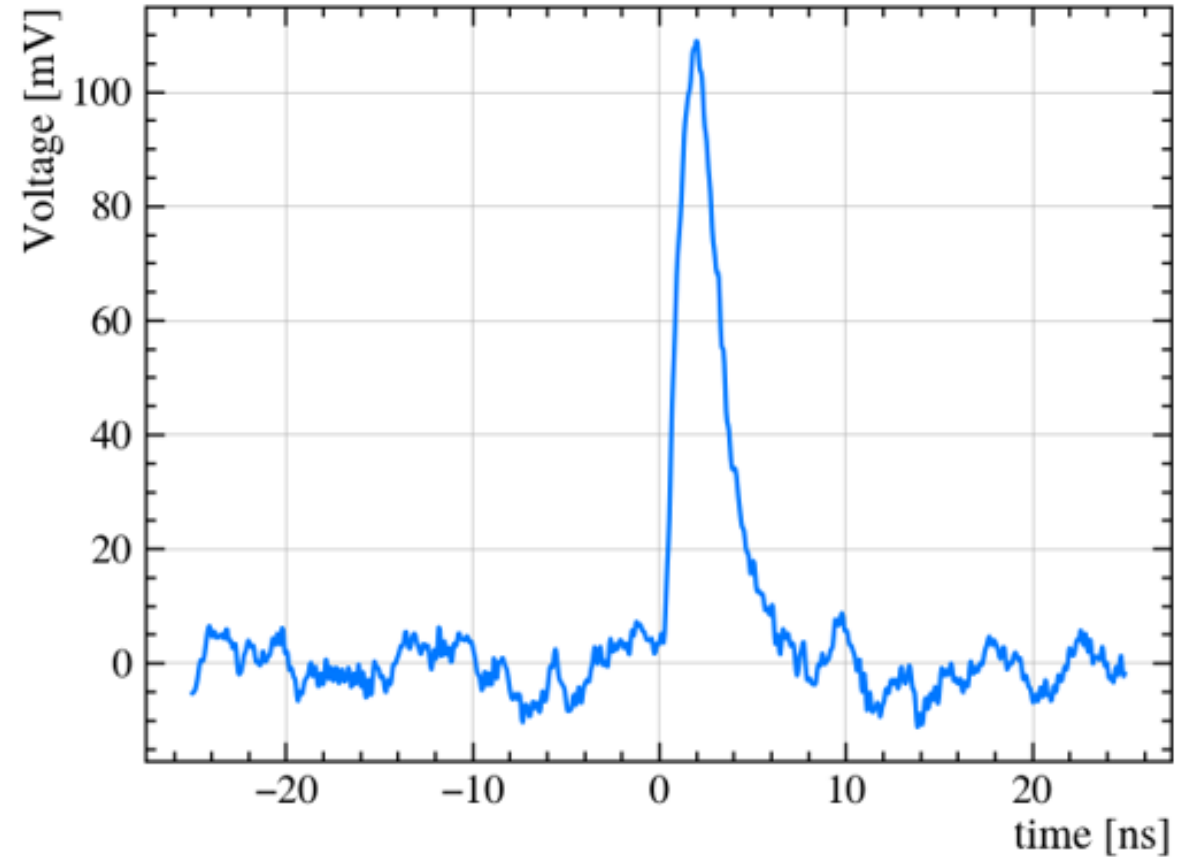
- The time-dependent weighting potential maps are computed through **COMSOL MultiPhysics**<sup>®</sup> ([www.comsol.com](http://www.comsol.com)) and the **Spectral Method**
- These maps are imported into **Garfield++** ([garfieldpp.web.cern.ch](http://garfieldpp.web.cern.ch)) through specific software components: **ComponentCOMSOL** and **ComponentVoxel**
- The **Heed** program as integrated in **Garfield++** is then used to simulate the interaction of the impinging particle with the sensor material
- Finally, in **Garfield++** the transport of charge carriers to the electrodes is simulated, which induces the output signal
- **At this point, the output signals from the sensor are obtained!!**



# READOUT AND NOISE EFFECTS

The signals produced by Garfield++ are:

- convoluted with the **transfer function of the readout electronics**
- resampled at the **oscilloscope's sampling frequency**
- and summed with **noise** from real noise events acquired with the oscilloscope



**FINAL SIGNAL READY TO BE ANALYZED!!**

Thanks to Kansas University Team and in particular to Nicola Minafra for developing and providing the boards.

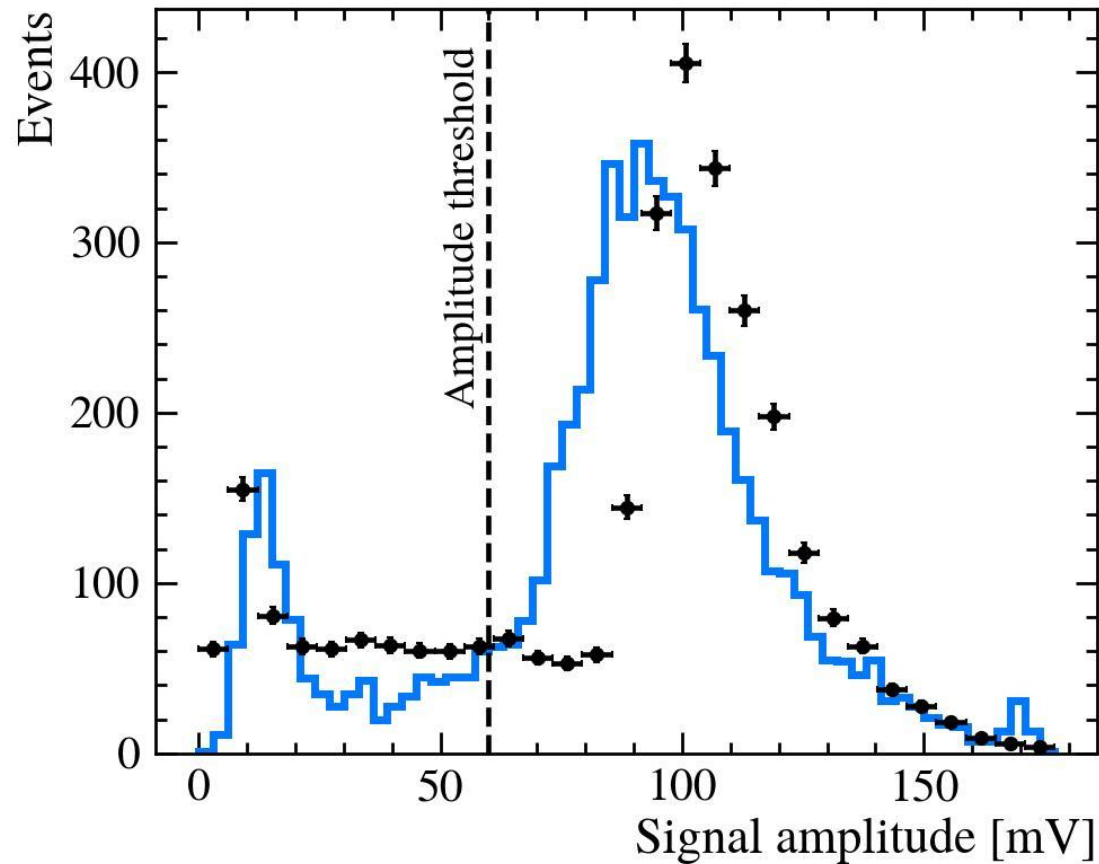


---

# **VALIDATION WITH EXPERIMENTAL DATA OF THE TEST BEAM AT SPS AT CERN IN 2021**

# COMPARISON OF THE AMPLITUDE DISTRIBUTIONS

$$A_{testb} = (89.7 \pm 0.4) \text{ mV}$$
$$A_{sim} = (101.7 \pm 0.6) \text{ mV}$$



## Distribution of amplitudes (maximum of the signal)

A **10% discrepancy** is observed probably due to the **underestimation of the resistance of the electrodes** of the beam test sensor.

## ELECTRODE RESISTANCE MEASUREMENT:

- **Sensor 1:** used in the beam test
- **Sensor 2:** has electrodes coming out on both sides, used to measure resistance; fabricated with the same parameters as Sensor 1

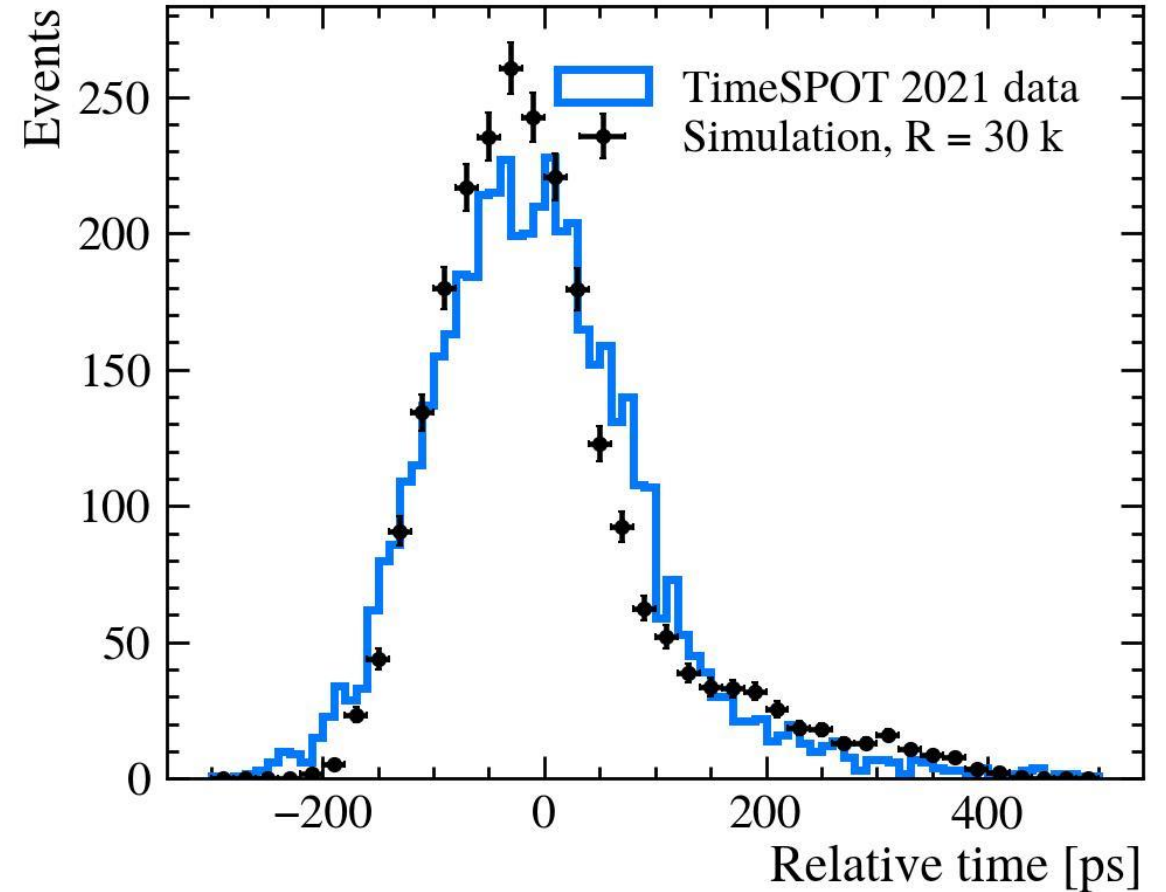
# COMPARISON OF THE TIME MARKERS DISTRIBUTIONS

$$\sigma_{t_{testb}} = (82 \pm 2) \text{ ps}$$
$$\sigma_{t_{sim}} = (71 \pm 3) \text{ ps}$$

## Distribution of time markers (obtained through a CFD with 30% threshold)

- Gaussian core: time resolution is evaluated as the width of the Gaussian core.

A **~10% discrepancy** is observed probably due to the **difference between amplitudes**.



---

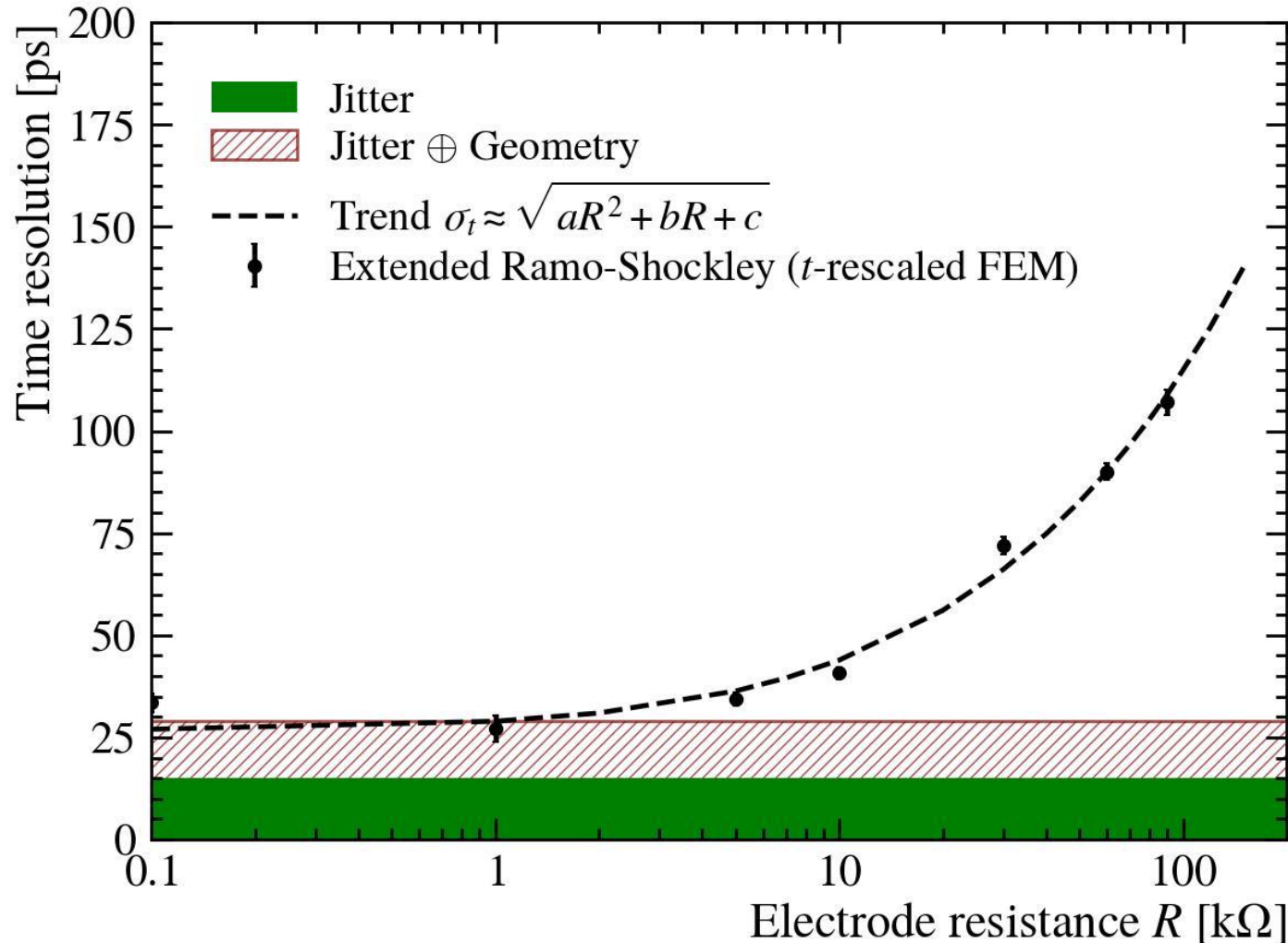
# OPTIMIZATION OF 3D DIAMOND DETECTORS BASED ON SIMULATION

The simulation reproduces the experimental data well enough to be used for the optimization of 3D diamond detectors:

- 1. EFFECT OF ELECTRODE RESISTANCE**
- 2. EFFECT OF TILTED DETECTOR**
- 3. OPTIMIZATION OF THE GEOMETRY**

# OPTIMIZATION OF 3D DIAMOND DETECTORS BASED ON SIMULATION

## 1. EFFECT OF ELECTRODE RESISTANCE

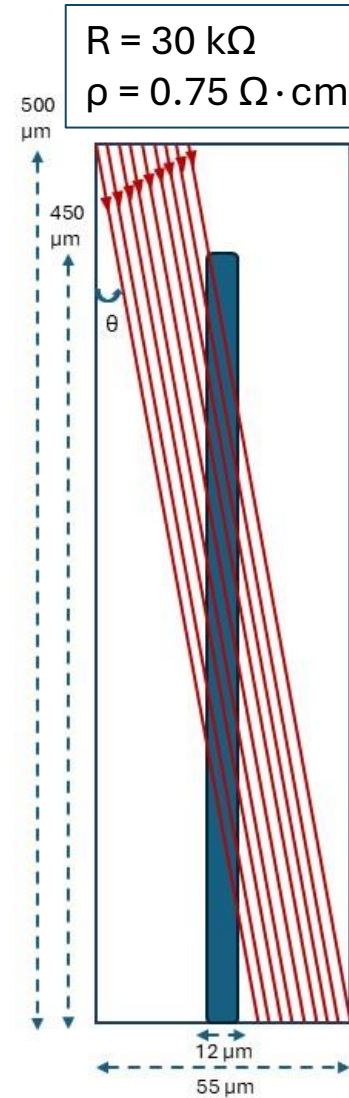
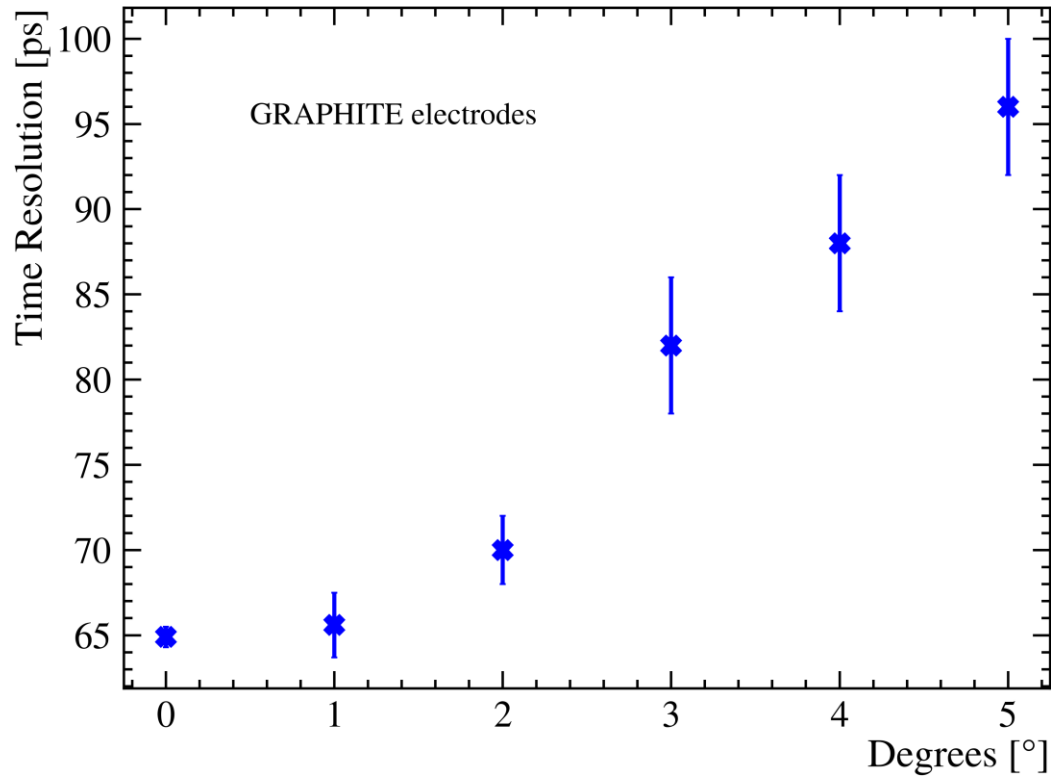


Dependence of the time resolution on the electrode resistance as predicted by scaling the time-dependence of the weighting potential.

Already with resistance of 10 k $\Omega$ , the contribution to the resolution from the resistance ( $\sigma_{resistance}$ ) becomes of the same order or subdominant with respect to the sum of the other components ( $\sigma_{distortion}$ ,  $\sigma_{jitter}$ )

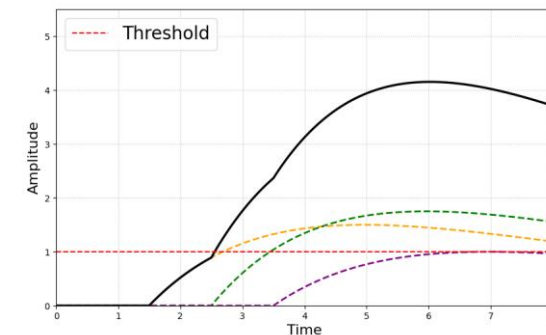
# OPTIMIZATION OF 3D DIAMOND DETECTORS BASED ON SIMULATION

## 2. EFFECT OF TILTED DETECTOR



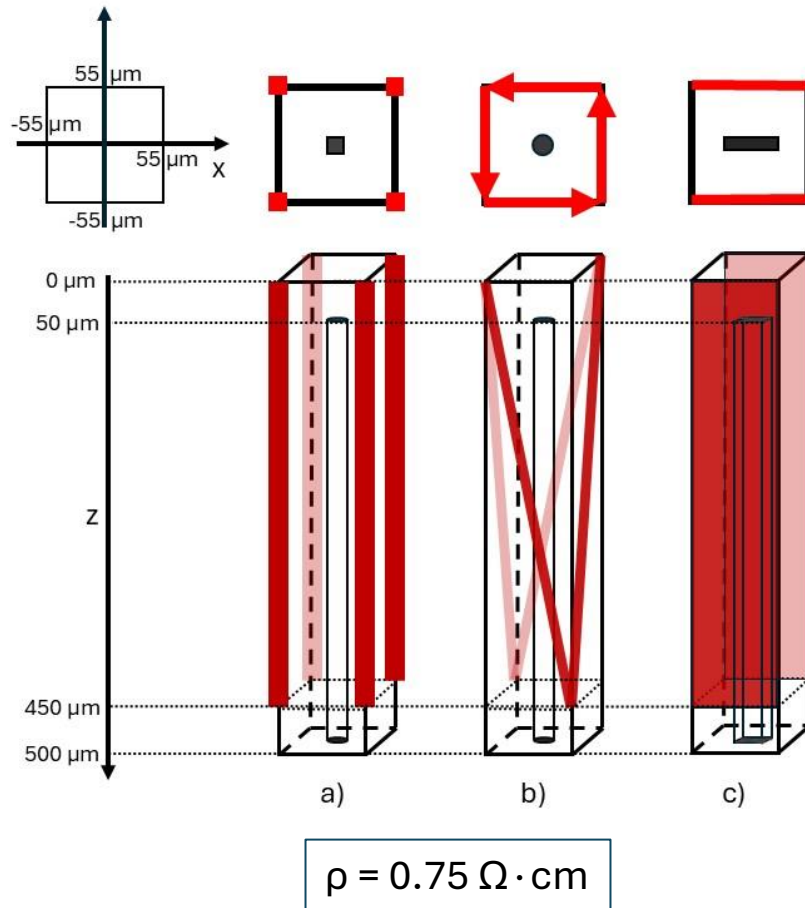
Time resolution as a function of the particle incidence angle on the detector. In principle, in detectors with electric field inhomogeneities, a slight tilt can be beneficial.

In this type of sensor, the improvement is not visible because of the presence of the resistance



# OPTIMIZATION OF 3D DIAMOND DETECTORS BASED ON SIMULATION

## 3. OPTIMIZATION OF THE GEOMETRY



The three electrode geometries considered are:

**a) Parallelepiped electrodes:** (square side  $11\ \mu\text{m}$ )

**b) Tilted electrodes:** Cylindrical polarization electrodes (diameter  $12\ \mu\text{m}$ ) are tilted (as proposed in VCI2025 Conference, CERN – see: [indico.cern.ch/event/1386009](https://indico.cern.ch/event/1386009))

**c) Trench electrodes:** This design emulates the geometry used in TimeSPOT silicon sensors

Sensor geometry	Time resolution [ps]	
	metallic electrodes	resistive electrodes
Default with cylindrical electrodes ( $\varnothing = 12\ \mu\text{m}$ )	$28 \pm 3$	$71 \pm 4$
Parallelepiped electrodes ( $11 \times 11\ \mu\text{m}^2$ )	$28 \pm 1$	$69 \pm 4$
Tilted electrodes ( $\varnothing = 12\ \mu\text{m}$ )	$26 \pm 3$	$69 \pm 4$
Trench electrodes	$22 \pm 2$	$50 \pm 3$

The contribution from the resistance is still dominant and prevents the time resolution from going below  $50\ \text{ps}$ , even with the trench geometry, which is, in any case, not feasible for diamond.

# CONCLUSION

---

- We have developed a simulation validated with the test beam to predict the design for optimization of the performance of these type of detectors
- From all the conducted studies the propagation of the signal along the electrode remains the dominant source of uncertainty in the determination of the time markers
- If the column resistance can be reduced to 10 k $\Omega$ , then all contributions to the time resolution must be carefully controlled to enable further improvements

# FUTURE DEVELOPMENTS

---

- Future work on this simulation will focus on its automation and on reducing the systematic uncertainties on the results due to the choice of the mesh
- Focus the future investigations on technological developments to reduce the resistivity for the traditional geometry with parallel columnar electrodes
- Optimization of the readout electronics should therefore proceed in parallel with the studies of improved geometries
- New experimental data to compare with!!!

---

**Thank you for your attention!**

---

# Backup slides

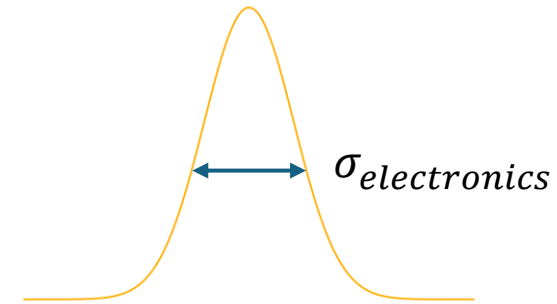
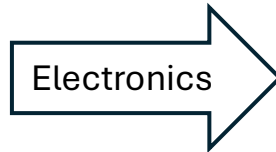
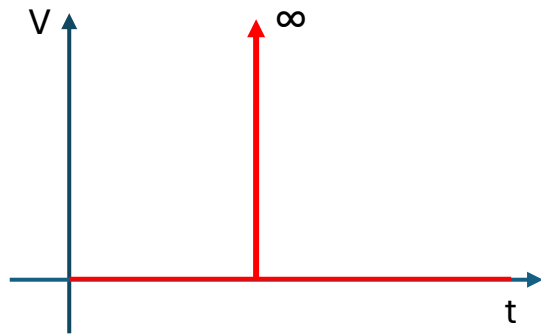
# JITTER CONTRIBUTIONS TO TIME RESOLUTION

Another important contribution to the time resolution is the one due to the jitter:

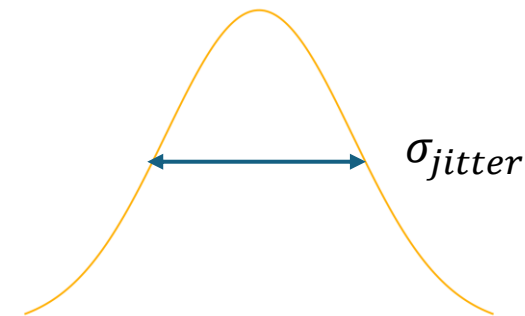
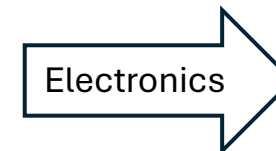
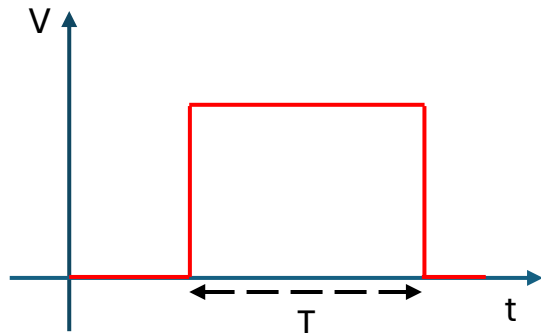
$$\sigma_{jitter} \propto \frac{N}{S/T} = \frac{T}{SNR}$$

$$\sigma_{jitter}^2 = \sigma_{electronics}^2 + \sigma_{carriers\_motion}^2$$

- $\sigma_{electronics}^2$  : contribute from pure electronics

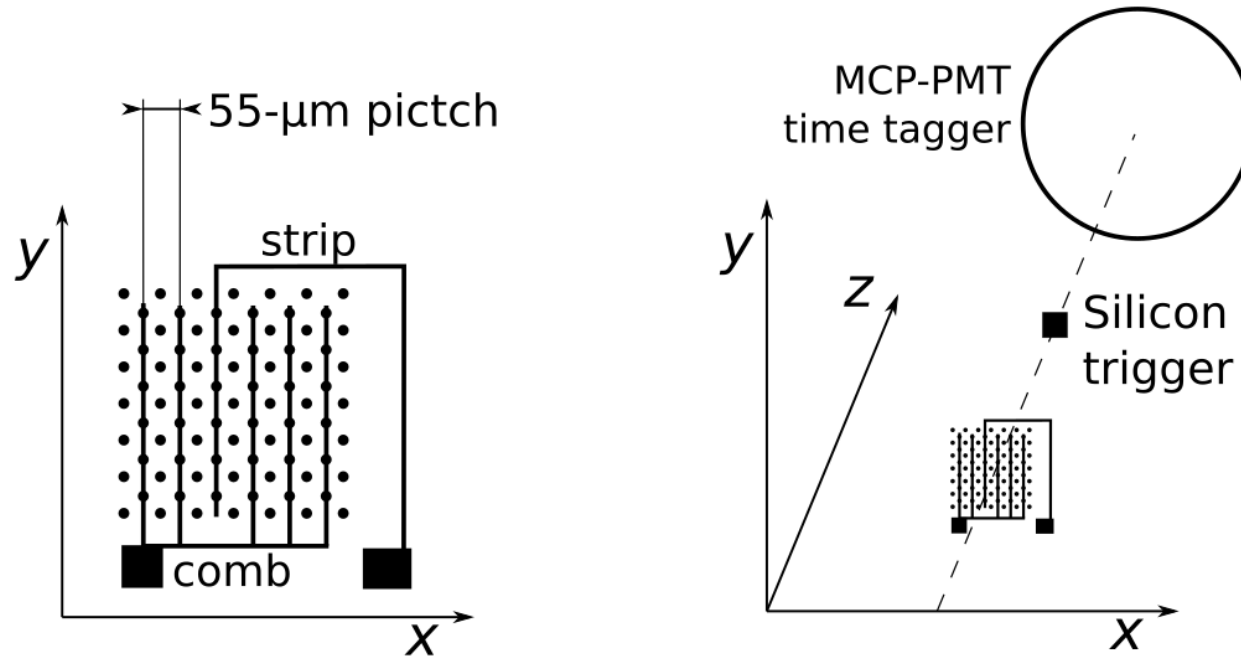


- $\sigma_{carriers\_motion}^2$  : contribute due to the sensor geometry, charge carriers have to reach the electrode in a finite time T



# TEST BEAM 2021

- The trigger condition is based on simultaneous signals observed in the silicon device and in a downstream MCP-PMT device acquired to provide precise time tagging of the impinging particles. The ultra-relativistic particles of the beam produce Cherenkov light in the quartz window of the MCP-PMT which is then detected providing time tags with uncertainties below 10 ps.



- Time resolution is computed on the time interval between two different time markers, set on a diamond structure and on the MCP used as time reference.

# EXTENSION OF RAMO-SHOCKLEY THEOREM

- **NOVEL APPROACH:**

**EXTENSION OF THE RAMO-SHOCKLEY THEOREM:** Effects of signal propagation due to impedance within the sensor can be modeled through a time-dependent weighting potential

$$\vec{i}_n = \frac{q}{V_w} \int_0^t \vec{E}_w(\vec{x}, t - t') \cdot \vec{v}(t') dt'$$

**Time-dependent weighting potential:** The time-dependent weighting potential solves the Maxwell equations in the quasi-static approximation:

$$\begin{cases} \nabla^2 V(\vec{x}, t) = -\frac{\rho(\vec{x}, t)}{\epsilon} \\ \vec{\nabla} \cdot (\sigma(\vec{x}) \vec{\nabla} V(\vec{x}, t)) + \frac{\partial \rho(\vec{x}, t)}{\partial t} = 0 \end{cases}$$

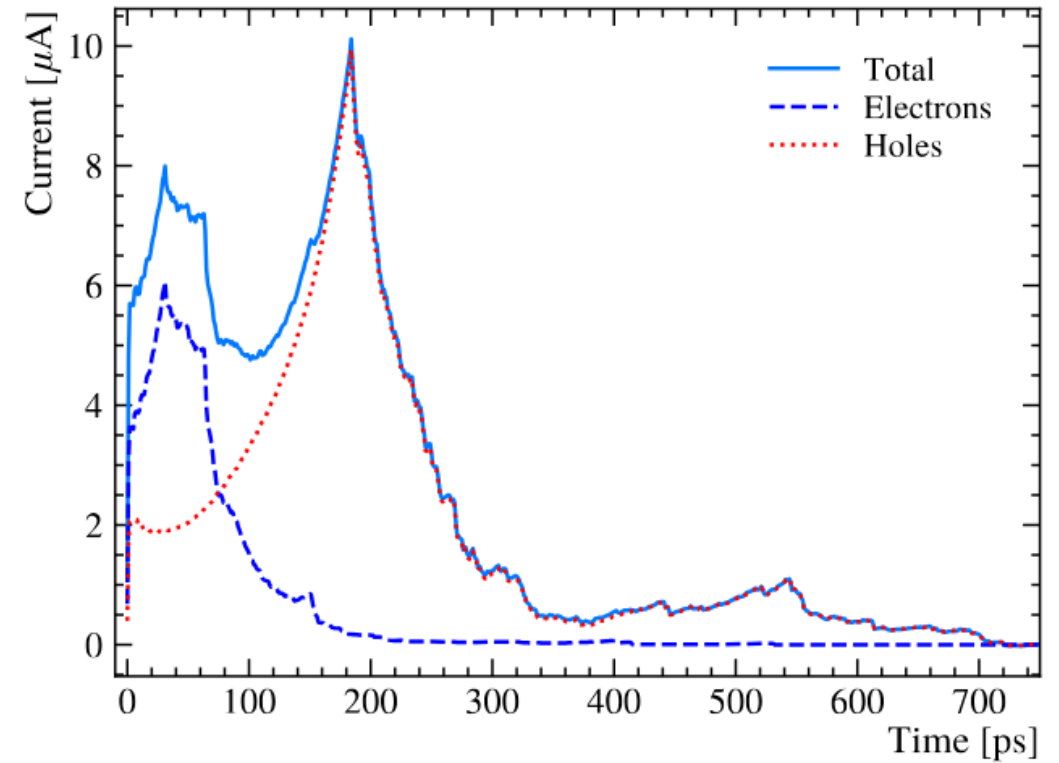
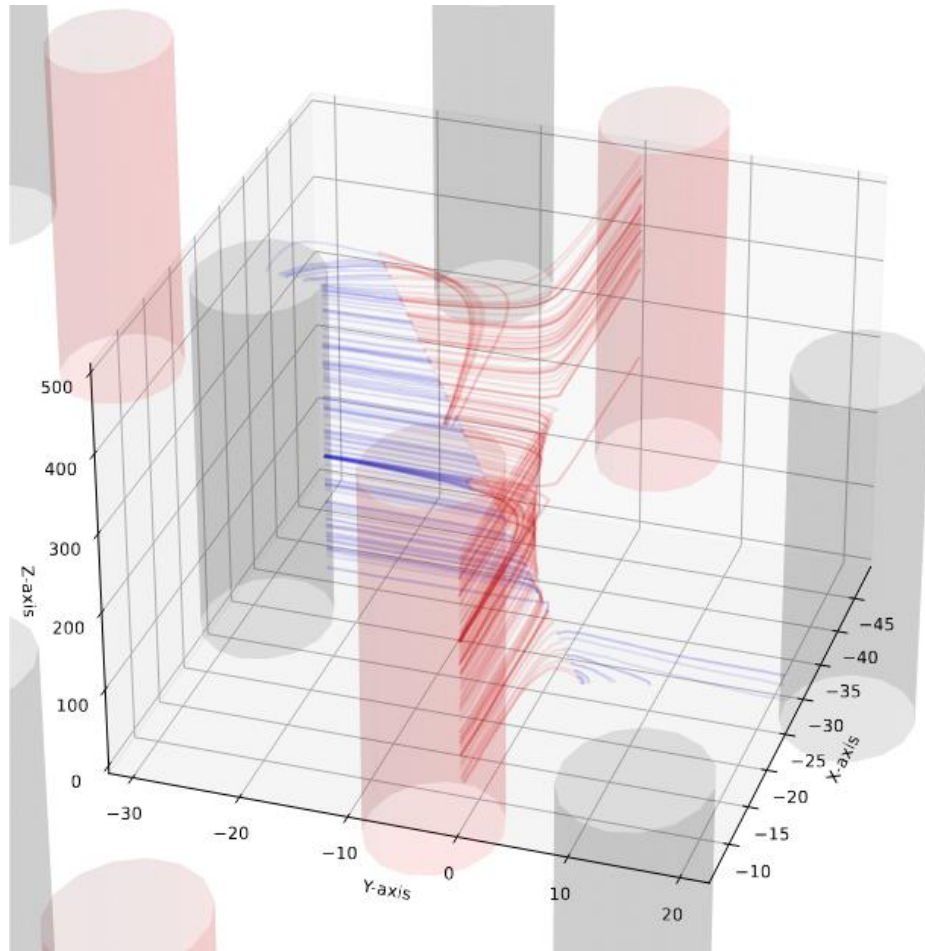
But the differential equation solved is a combination through Poisson and continuity equations:

$$\frac{\partial}{\partial t} \nabla^2 V(\vec{x}, t) - \frac{1}{\epsilon} \vec{\nabla} \cdot (\sigma(\vec{x}) \vec{\nabla} V(\vec{x}, t)) = 0$$

➤ Invariance

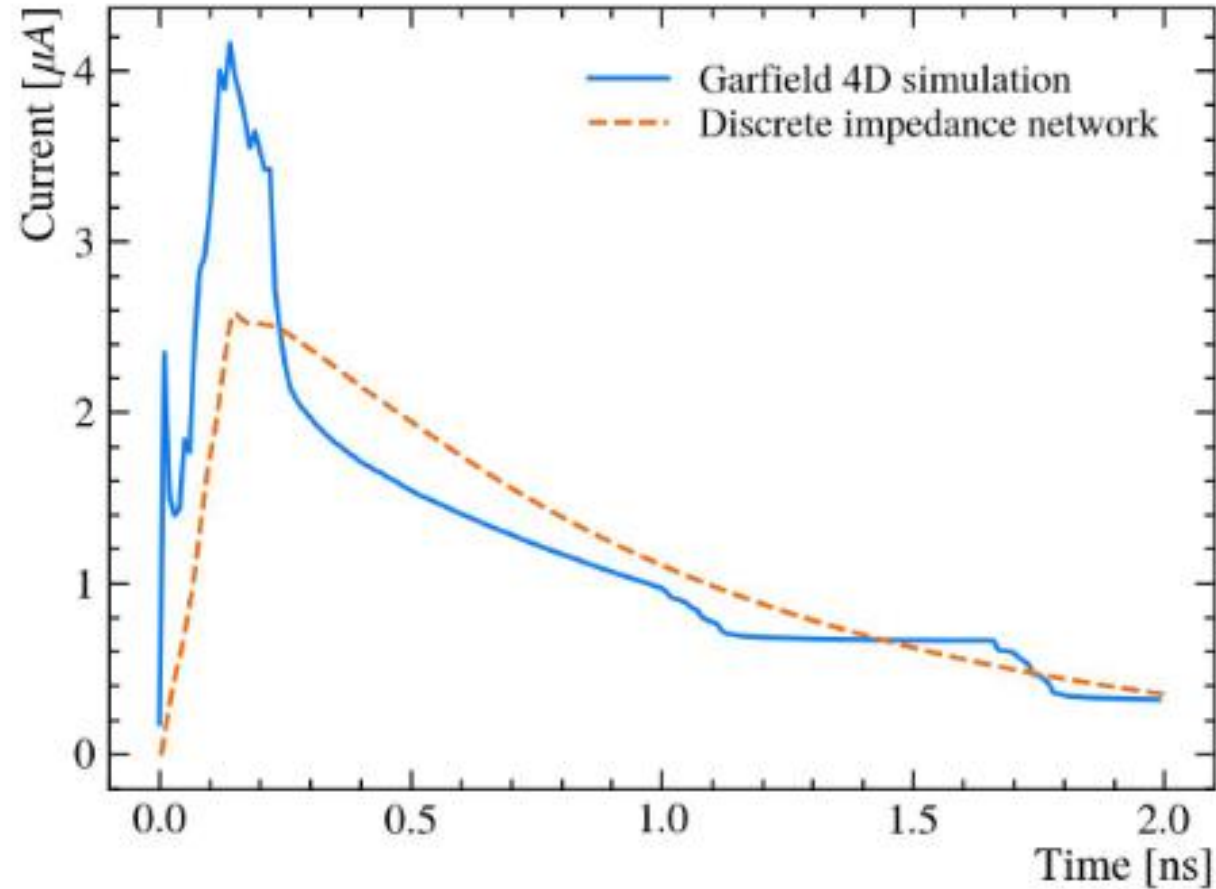
$$V\left(\vec{x}, \frac{t}{\alpha}; \alpha \sigma(\vec{x})\right) = V(\vec{x}, t; \sigma(\vec{x}))$$

# TOTALLY METALLIC ELECTRODES



# COMPARISONS

## COMPARISON BETWEEN OLD APPROACH AND NOVEL APPROACH IN THE CASE OF 3D GRAPHITIC COLUMNAR ELECTRODES



# COMPARISONS

## COMPARISON BETWEEN ALL THE APPROACHES RESULTS IN THE CASE OF 3D GRAPHITIC COLUMNAR ELECTRODES

